Optimizing Diol Hydroxyl Fraction within a Diol–Triol Polyol System and Chain-Extender Hydroxyl Fraction to Balance Mechanical Strength and Flexibility in Two-Component Polyurethane Roof Coatings

A. Eshraghi [1*], M.R. Foruzanmehr[2],

[1,2] Department of Civil Engineering, University of Ottawa, Ottawa, Canada

*aeshr088@uottawa.ca

Keywords: *Polyurethane roof coatings, Diol-triol polyol hydroxyl fractions, Chain extender hydroxyl fractions*

1. Abstract

Two-component solvent-free polyurethane (PU) coatings are widely used as waterproofing membranes for flat roofs; however, optimizing their formulation to simultaneously achieve mechanical strength, flexibility, and water resistance remains challenging. In this study, nine thermoset PU formulations were prepared by systematically varying the diol hydroxyl fraction within a diol–triol polyol system and the chain-extender OH fraction relative to the total hydroxyl groups. Viscoelastic properties were characterized by DMA, and tensile properties were evaluated in accordance with ASTM D412. Increasing the fraction of hydroxyl groups originated from chain-extender promoted microphase separation, resulting in higher storage modulus and tensile strength. However, its effect on elongation at break did not follow a simple increasing or decreasing trend, with the highest elongation observed at the intermediate chain-extender hydroxyl fraction (0.6). Reducing the hydroxyl groups originated from diol polyol fraction within the diol–triol polyol system, which corresponded to the increased in the fraction of the hydroxyl groups originated from triol polyol, and higher chemical crosslinking density, improved tensile strength, and storage modulus. Elongation at break was lowest at the intermediate diol polyol hydroxyl fraction (50%), likely due to structural heterogeneity, and highest at the lowest diol polyol hydroxyl fraction (30%). Together, these findings provide a systematic strategy for optimizing thermosetting polyurethane formulations with balanced mechanical strength, and flexibility for roof coating applications.

2. Introduction

Roof coatings form a continuous protective layer over roofing substrates, protecting them from water penetration, ultraviolet radiation, and environmental degradation, thereby extending roof service life. Inadequate waterproofing, especially on low-slope and flat roofs, can lead to leakage, mould growth, corrosion, and eventually roof failure. Traditionally, waterproofing in low-slope roofing has commonly relied on bituminous membranes, including built-up roofing systems and modified bitumen membranes such as APP- and SBS-modified bitumen [1]. However, studies have shown that bitumen sheets may exhibit dimensional instability, lap-joint defects, and loss of surface mineral protection, leading to cracking, reduced waterproofing performance, and an increased risk of water infiltration in flat roofs [2], [3].

To address these limitations, liquid-applied roof waterproofing systems (LARWS) have become an important alternative. They form seamless, fully adhered membranes that minimize water ingress. These systems include polymer-modified cementitious coatings, acrylic dispersions, silicone coatings, liquid rubber emulsions, and polyurethane-based systems [4]. LARWS can be applied at room temperature, adapt to irregular roof geometries, and avoid the fire hazards and installation challenges of heat-applied bitumen. However, their mechanical strength and long-term durability depend primarily on the polymer type, which is critical for pedestrian-accessible roofs and harsh environmental conditions [4]. Polyurethane (PU)-based liquid-applied membranes are widely known as high-performance systems because they offer superior mechanical strength, flexibility, and durability compared with acrylic, silicone, or PMMA coatings [4], [5]. Two-component polyurethane (2K PU) systems, which cure through a polyaddition reaction between a polyol blend (Part A) and a polyisocyanate (Part B), form dense, crosslinked elastomeric networks with high chemical resistance. Most 2K PU roof coatings are solvent-free, which is beneficial for eliminating volatile organic compound emissions, reducing shrinkage, and minimizing odour and fire risk during application [5], [6], [7].

Polyurethanes are segmented block copolymers composed of soft segments derived from polyols, which provide flexibility, and hard segments formed from the reaction of diisocyanates and chain extenders, which are responsible for the mechanical strength and dimensional stability. Thermodynamic incompatibility between soft and hard segments leads to microphase separation, resulting in the formation of hard domains that act as physical crosslinks in a soft matrix [8]. The functionality of the polyol and isocyanate determines whether the system is thermoplastic or thermosetting; multifunctional components promote chemical crosslinking, which enhances dimensional stability, mechanical strength, and resistance to water uptake [9], [10]. One of the main challenges in designing polyurethanes for specific performance requirements is that their final properties are governed by many interconnected formulation parameters, including the type and molecular weight of the polyol, the type of isocyanate, the structure and content of the chain extender, the hard-to-soft segment ratio, the degree of microphase separation, and the chemical crosslinking density. These parameters do not act independently but interact simultaneously, often producing competing effects on the final material properties [11], [12]. The literature provides clear evidence of how sensitive PU properties and microstructure are to changes in each of these parameters.

Regarding polyol type, Bagdi et al.[13] showed that replacing polyether polyols with polyester polyols promoted more developed microphase separation between hard and soft segments, leading to a higher tensile strength and stiffness; however, polyether-based systems showed better

hydrolytic stability and flexibility, indicating how the choice of polyol creates a trade-off between mechanical performance and durability when the material is exposed to water. In terms of polyol molecular weight effects, Silver et al. [14] demonstrated that increasing the polyol molecular weight in PEG-based polyurethane elastomers increased the degree of phase separation and crystallinity, while also increasing tensile strength and water absorption. However, elongation at break reached a maximum at the intermediate PEG molecular weight, indicating that no single polyol molecular weight simultaneously optimized strength, extensibility, and water resistance. The choice of isocyanate shows the same trade-off , Wang et al. [15] showed that aromatic MDI-based polyurethanes developed stronger inter-segment hydrogen bonding and more organized hard domains, resulting in higher modulus and glass transition temperature, whereas aliphatic HDI- and IPDI-based systems produce softer, more flexible networks with better weathering resistance but lower mechanical performance. In terms of the effects of the chain extender choice and content Tan et al. [16] found that linear chain extenders promoted stronger hard–soft phase separation and higher mechanical performance compared with branched extenders, which yielded more mixed morphologies and reduced stiffness. They also showed that increasing the chain extender fraction relative to total reactive OH groups increased the degree of microphase separation and raised mechanical performance, but this comes at the cost of reduced flexibility, as a higher chain extender content increases hard-segment proportion and restricts soft-segment mobility creating a direct trade-off between stiffness and elongation[16]. In terms of the effect of hard segments content, Liu et al. [17] showed that increasing hard-segment content enhanced microphase separation and hydrogen bonding, increasing the storage modulus in the rubbery plateau, but also reduced chain mobility and caused brittle failure at high hard-segment fractions. The effect of chemical crosslinking on polyurethane properties has also been widely demonstrated in literature. Barros et al.[18] demonstrated that introducing a triol crosslinker increased tensile strength but simultaneously suppressed hard-segment crystallinity by restricting chain mobility, again showing the trade-off nature of polyurethane formulation, where improving strength through increased crosslinking may compromise molecular organization or flexibility. Similarly, Trzebiatowska et al. [19] reported that increasing crosslink density increased tensile strength, storage modulus, elastic modulus, and hardness, but decreased elongation at break. This reduction in elongation can be explained by the higher density of crosslinking points, which restricts soft-segment mobility and limits the ability of polymer chains to stretch before failure.

For roof coating applications, the membrane must simultaneously satisfy various performance requirements such as sufficient mechanical strength, particularly resistance to dynamic and static indentation, depending on the level of foot traffic expected on the roof [1], [4]; adequate flexibility to accommodate structural deformations without cracking[1]; and low water absorption to maintain long-term waterproofing integrity[1]. Achieving this combination of properties in a single formulation is particularly challenging because the structural features that improve one property often compromise another. From the previous studies it can be concluded that higher crosslink density reduces water absorption but limits elongation; stronger hard domains improve strength but reduce flexibility; and a more dominant soft-segment matrix improves ductility but increases water ingress. As a result, the three target properties pull the formulation in different directions simultaneously. Despite this, most existing studies on polyurethane waterproofing membranes have focused on evaluating specific formulations or installed waterproofing systems rather than systematically navigating formulation trade-offs [20]. Therefore, detailed studies that connect formulation variables to the balance between mechanical strength, and flexibility in liquid-applied roof membranes remain limited.

A further limitation of most polyurethane studies is that formulations are described using weight fractions, which do not directly reflect the stoichiometry of reactive functional groups. For instance, Huang et al. [21] varied hard-segment content at 40, 45, and 50 wt% to study its effect on microphase structure and mechanical performance; Yan et al. [22] similarly defined hard-segment content in weight percent when investigating its effect on microphase separation and tensile strength. Since various polyols and chain extenders differ in molecular weight and functionality, weight fraction alone does not fully indicate the number of reactive OH groups contributing to network formation. Kosanovich et al. [23] showed that triols with lower hydroxyl equivalent weight (HEW), meaning more reactive OH groups per gram of polyol, required more isocyanate to maintain the NCO/OH stoichiometric balance, resulting in higher crosslink density and altered coating properties. This approach, however, has rarely been used as a primary formulation tool. Tan et al. [16] and Barros et al. [18] applied similar concepts and demonstrated clear effects on microphase separation and mechanical properties, but systematic application to roof coating formulation remains absent from the literature.

To address these gaps, this study aimed to develop a formulation window by simultaneously tuning two key parameters: chemical crosslink density and microphase separation. For this purpose, two hydroxyl-fraction-based ratios were defined: the fraction of the hydroxyl groups originated from diol polyol in a diol-triol polyol system which controls the fraction of hydroxyl groups contributing to chemical crosslinking, and the fraction of the hydroxyl groups originating from chain extender relative to the total hydroxyl groups existing in the system, which controls the amount of hydroxyl groups available for the isocyanate groups to form hard-segments. In this case, a higher contribution of chain-extender OH groups can lead to greater hard-segment formation through reaction with isocyanate, thereby shifting the balance between mechanical strength, and flexibility. By studying these two ratios together, this work aimed to identify the optimized ratio combination that provides the best balance between mechanical strength, and flexibility required for liquid-applied polyurethane roof coating applications.

3. Experimentation

3.1. Materials

polytrimethylene ether glycol-type polyether diol (PO3G, Mn = 2600–2800 g mol^{-1}, Product No. 923982, Sigma-Aldrich, USA) was used as the soft-segment diol polyol, and castor oil provided by Sigma-Aldrich, USA served as the triol polyol to introduce crosslinking. 1,4-Butanediol (≥99%, Sigma-Aldrich, USA) was used as the chain extender, and Basonat HI 2000 NG (BASF, Germany), an HDI-based polyisocyanate (functionality >2), was used as the isocyanate component. Dimethyltin dichloride (97%, Sigma-Aldrich, USA) was employed as the catalyst, and ethylenediamine tetrakis(ethoxylate-block-propoxylate) tetrol (average Mn = 7200 g mol^{-1}, Product No. 435546, Sigma-Aldrich, USA) was added as a defoamer to reduce bubble formation. All materials were used as received.

3.2. Design of Diol/Triol Polyol Ratios and Chain Extender OH Fraction

The diol hydroxyl fraction in the diol–triol polyol system was set at 80%, 50%, and 30%. These values indicate the percentage of polyol hydroxyl groups supplied by the diol polyol, while the remaining hydroxyl groups were supplied by the triol polyol. Therefore, the three levels represent high-diol, intermediate diol, and low-diol systems, respectively. The chain-extender hydroxyl

fraction was set at 0.3, 0.6, and 0.9, representing the fraction of the hydroxyl groups originating from chain extender relative to the total hydroxyl groups in the system. For example, a value of 0.3 means that 30% of the total hydroxyl groups originated from the chain extender, while the remaining 70% originated from the combined diol–triol polyol system. Similarly, 0.6 and 0.9 correspond to 60% and 90% chain-extender hydroxyl contribution, respectively. Across all formulations, the isocyanate-to-hydroxyl group ratio was kept constant at 1.05, and the resulting nine formulations are summarized in Table 1.

Table 1 Summary of the different formulations used for preparation of the samples with varying diol/triol and chain extender ratios.

Sample	Diol Polyol OH Percentage (%)	Triol Polyol OH Percentage (%)	Chain-Extender OH fraction	Hard Segment content (%)
80-0.9	80	20	0.9	66.81
80-0.6	80	20	0.6	32.19
80-0.3	80	20	0.3	20.31
50-0.9	50	50	0.9	73.28
50-0.6	50	50	0.6	39.26
50-0.3	50	50	0.3	25.78
30-0.9	30	70	0.9	78.34
30-0.6	30	70	0.6	46.04
30-0.3	30	70	0.3	31.41

3.3. Sample Preparation

For the preparation of the two-component polyurethane samples, polytrimethylene ether glycol diol, castor oil, 1,4-butanediol chain extender, ethylenediamine tetrakis(ethoxylate-block-propoxylate) tetrol defoamer (1 wt% relative to total formulation weight), and dimethyltin dichloride catalyst (0.125 wt% relative to total formulation weight) were added to a clean polypropylene beaker in amounts determined by each formulation composition and mixed with a mechanical stirrer at 50 rpm for 3 minutes to ensure uniform blending. The defoamer and catalyst were kept constant across all formulations. The resulting polyol mixture (Part A) was then combined with the HDI-based isocyanate (Part B), mixed at 50 rpm for 1 minute to obtain a homogeneous mixture, immediately poured into silicone molds, and cured at room temperature until FTIR confirmed the absence of unreacted NCO groups

3.4. Characterization Techniques

3.4.1. Dynamic Mechanical Analysis

The dynamic mechanical properties of the samples were measured in tension-film mode using a TA Instruments Q800 DMA. The samples were heated from −60 to 80°C at a heating rate of 3°C/min under a constant frequency of 10 Hz. This frequency was selected based on the characterization of the linear viscoelastic region. The oscillation amplitude was set to 15 µm, with a preload force of 0.1 N. The storage modulus (E′), loss modulus (E″), and loss factor (tan δ) were

recorded as functions of temperature. Glass transition temperature (Tg) was determined as the temperature corresponding to the peak of the tanδ curve.

3.4.2. Tensile Test

Tensile properties of the samples were evaluated using a universal testing machine (Instron 68FM-100). Dog-bone specimens were tested using a 1 kN load cell at room temperature, following ASTM D412. The crosshead speed was set to 10 mm/min. Tensile strength and elongation at break were recorded.

4. **Results and Discussion**

4.1. DMA Analysis

Dynamic mechanical analysis was conducted to evaluate the viscoelastic behavior and microstructure of the samples. Fig 1. shows the results for storage modulus of the samples with different formulations. The results showed that, at a constant diol/triol composition, increasing the chain-extender ratio increased the storage modulus across the entire temperature range. This trend is observed both below the glass-transition region and at elevated temperatures. Increasing the chain-extender ratio increased the fraction of hard segments, which act as physical crosslinks that restrict chain motion, and consequently led to a higher storage modulus [24].

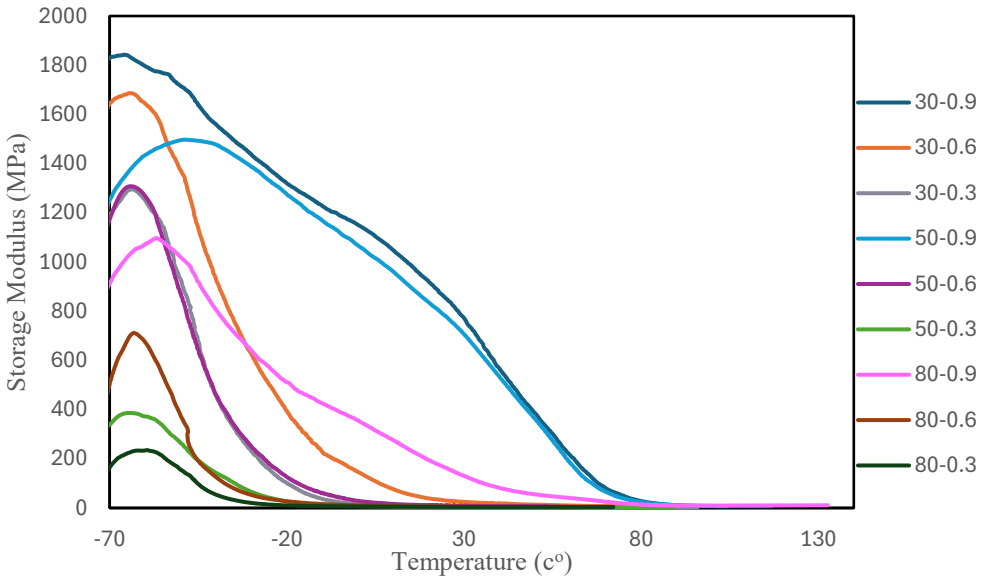

Fig 1. Storage modulus of the samples with different formulations obtained from DMA analysis.

Table 2 Summary of the temperature corresponding to the tan delta peak across all the formulations

Sample	Temperature Corresponding to The First Tan Delta Pek	Temperature Corresponding to The Second Tan Delta Pek
80-0.3	-39.7	-

80-0.6	-49.5	53.7
80-0.9	-56.8	76.8
50-0.3	-20.4	-
50-0.6	-14.9	57.9
50-0.9	-50.2	76.8
30-0.3	-2.7	-
30-0.6	12.7	53.8
30-0.9	-65.9	-81.1

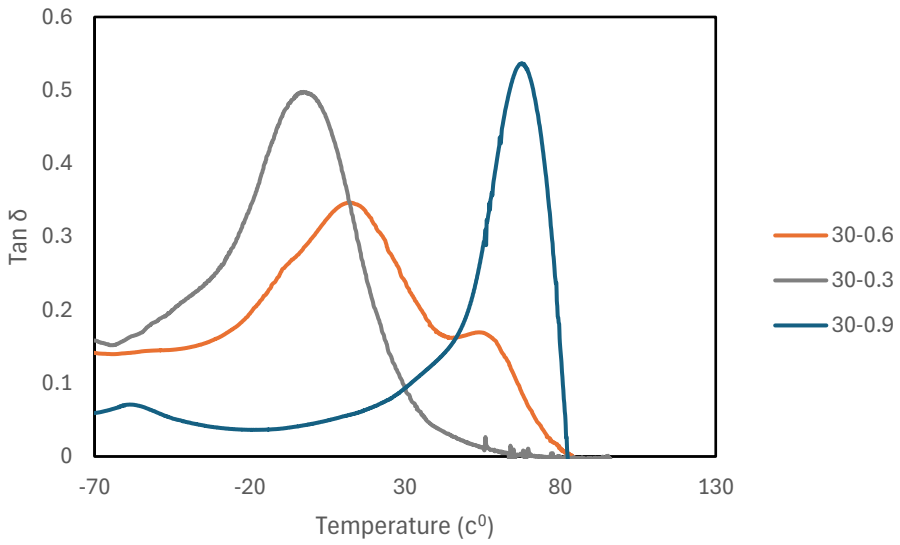

Figure2. Tan delta graphs across samples with 30% diol hydroxyl group fraction and varying hydroxyl fractions originating from chain extender.

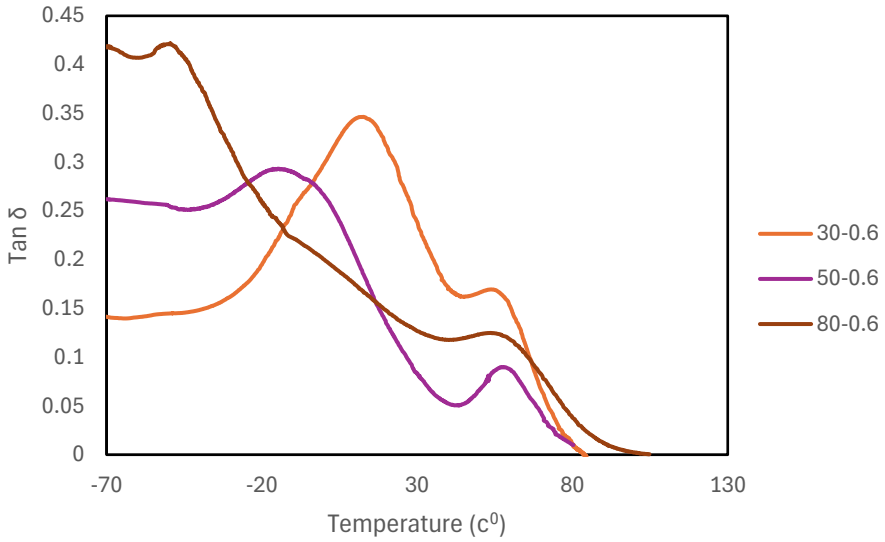

Figure3. Tan delta graphs across samples with the intermediate chain extender originated hydroxyl group fraction(0.6) and varying diol originated hydroxyl fractions.

The DMA results showed that, in formulations with low and medium chain-extender hydroxyl fractions (0.3 and 0.6), the storage modulus dropped rapidly with temperature and then reached a rubbery plateau. In contrast, systems with high chain-extender content exhibited a more gradual decrease in modulus and do not reach their rubbery plateau within the investigated temperature range, indicating a stiffer network with more effective physical crosslinking arising from the thermodynamic incompatibility between hard and soft segments which leads to microphase separation, causing hard segments to aggregate into ordered domains that act simultaneously as physical crosslink points and reinforcing fillers embedded in the soft matrix. This is consistent with Yang et al.[25] who reported that increasing hard-segment content increases hydrogen bonding density within hard domains, restricting molecular motion and elevating storage modulus. In addition, at a fixed chain-extender level, reducing the diol polyol hydroxyl fraction (and increasing the triol fraction) increased the storage modulus across the entire temperature range. This reflects the higher chemical crosslinking density introduced by the triol component. Unlike difunctional diols, which form linear chain extensions, the three hydroxyl groups of castor oil react with isocyanate groups to create covalent branch points that permanently tie polymer chains together into a three-dimensional network, restricting segmental mobility and raising modulus.

The tan δ peak was considered as an indicator of the glass transition temperature (Tg). Table 1 summarizes the temperature corresponding to the tan δ peaks across all the formulations. As shown by the DMA tan δ curves and table1, increasing the chain-extender ratio generally promoted microphase separation in the polyurethane samples. As the chain-extender OH fraction increases, a greater proportion of the total reactive OH groups are contributed by the chain extender rather than the polyols. Since chain extender OH groups react with isocyanate to form urethane linkages within hard segments, a higher chain-extender fraction directly increases hard-segment content and concentration. As hard segments increase, a more developed microphase separation is formed. The DMA results indicated that the sample with the lowest chain-extender ratio showed only one

tan δ peak at low temperatures which was only assigned to the relaxation of the soft segments. The absence of a second distinct tan δ peak at higher temperatures, which would be expected from the relaxation of well-developed hard domains, indicates limited or no microphase separation in these formulations. suggesting limited or no microphase separation. This is likely because the chain-extender content was insufficient to form distinct hard domains, resulting in small and poorly organized hard-segment domains. In contrast, the sample with an intermediate chain-extender ratio (0.6) showed a main tan δ peak with a shoulder at slightly higher temperatures. This shoulder suggests the development of an additional relaxation process, indicating the beginning of more distinct microphase-separated regions within the material. This finding is consistent with Velankar and Cooper [26], who reported that a shoulder in the tan δ curve can be an important sign of microphase separation in polyurethane systems. This shoulder suggests the presence of an additional relaxation process, likely related to the development of hard-segment-rich domains within the softer polyurethane matrix. For the samples with the highest chain extender ratio (0.9), a clearer separation of relaxation processes is observed for all crosslinking densities. In these samples, a small peak appears in the low-temperature range (approximately −60 to −50 °C), while a larger and sharper peak is observed at higher temperatures between about 50 and 70 °C and the temperature difference between these two peaks is significantly larger compared with the samples containing the medium chain extender ratio. This trend suggests that increasing the chain extender ratio enhances the degree of microphase separation within the polyurethane network [27].

As the fraction of diol polyol hydroxyl groups decreased, the low-temperature tan δ peak associated with the soft-segment glass transition shifted to higher temperatures. This shift indicates that the mobility of the soft segments became more restricted. This can be explained by the simultaneous increase in the fraction of the hydroxyl groups originating from the triol polyol in the polyol blend. The trifunctional triol creates covalent branch points within the network and connects the soft segments at several points. As a result, when the hydroxyl fraction of the diol polyol decreased and the hydroxyl fraction of the triol polyol increased the chemical crosslink density increased, the soft-segment chains become less free to move because they are held more tightly within the network. Therefore, more thermal energy is needed for these chains to move, causing the glass transition to shift to higher temperatures. The same increase in chemical crosslink density also caused the observed reduction in microphase separation as the diol hydroxyl fraction decreased. The formation of well-defined hard domains requires hard segments to have sufficient mobility to diffuse, aggregate, and organize into ordered structures within the soft matrix which is governed by segmental diffusion. As the triol hydroxyl fraction increased and more covalent crosslinks were introduced into the network, this diffusion became progressively more restricted, limiting the ability of hard segments to rearrange and assemble into distinct domains. This is reflected in the tan δ curves: for example, for the intermediate chin extender hydroxyl fraction (0.6) at the highest diol hydroxyl fraction (80%), two distinct peaks were observed for the soft- and hard-segment relaxations, indicating well-developed microphase separation with clearly defined hard domains. As the diol fraction decreased to 50%, one main peak and a shoulder-like feature were observed rather than two distinct peaks, and both features became broader. This broadening indicates a more heterogeneous microstructure, some hard segments retained sufficient mobility to form partial hard domains, while others remained dispersed within the soft matrix, resulting in a wide distribution of local environments and relaxation times. Therefore, the 50% diol hydroxyl fraction formulations represented the most heterogeneous case. In this case, chemical crosslinking density formed by introducing more hydroxyl groups originated form the triol polyol, was high enough to partially restrict hard-domain formation compared to the 80% diol

case, yet not high enough to prevent it entirely. At the lowest diol hydroxyl fraction (30%), the crosslink density was sufficiently high to restrict hard-segment diffusion more than the 50%,diol polyol hydroxyl fraction preventing aggregation into distinct domains. As a result, hard segments are more dispersed within the soft matrix, producing a more homogeneous though heavily constrained microstructure.

4.2. Tensile Test

The tensile results (Fig 3–4.) showed that, at constant fraction of hydroxyl groups originating from diol polyol, increasing the chain-extender ratio increased tensile strength due to the formation of more hard segments that act as physical crosslinks, reinforcing the structure. However, elongation at break reached a maximum at the medium chain-extender level. At low chain-extender contents, few hard domains were present, and the network was weakly connected, leading to low strength and only moderate elongation. At medium chain-extender contents, the morphology was more balanced, which means that the hard domains provided physical crosslinks while the soft phase remained deformable, resulting in the highest elongation and toughness. At high chain-extender contents, dense hard-segment associations strongly restricted chain mobility which increased the mechanical strength but also caused brittle failure.

Changing the fraction of hydroxyl groups originating from the diol polyol led to a non-linear behavior in elongation at break. The formulations with the intermediate fraction of hydroxyl groups origination from the diol polyol (50) showed the lowest elongation across all the chain extender hydroxyl fractions. This trend is likely because of the heterogeneous structure observed within these formulations and the broad tan delta peaks in DMA results confirmed it. Decreasing the fraction of hydroxyl groups originating from the diol polyol to its lowest level (30%) and correspondingly increasing the hydroxyl fraction originating from the triol polyol, introduced a higher density of hydroxyl groups capable of forming chemical crosslinks. As the DMA results showed, this case exhibited the lowest degree of microphase separation. As a result, rather than a distinctly microphase-separated morphology, the hard segments were dispersed within the soft-segment matrix, producing a more uniform network. Therefore, the high elongation at break observed in these samples can be attributed to the uniform microstructure that they have compared to the other formulations.

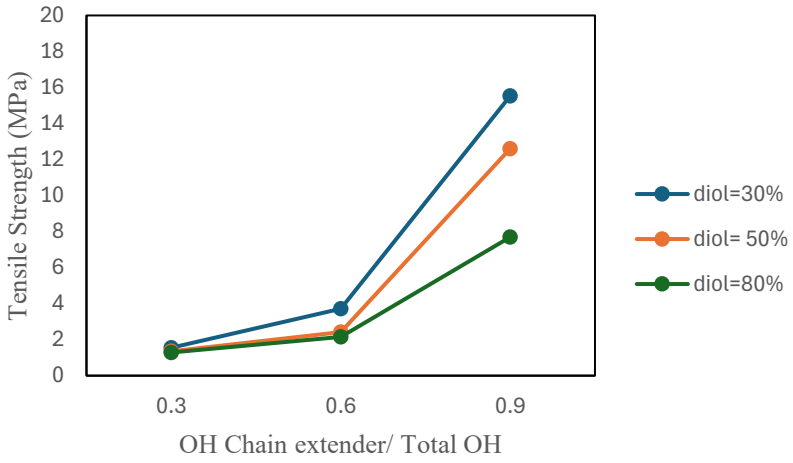

Figure 4. Tensile strength of the samples with different formulations.

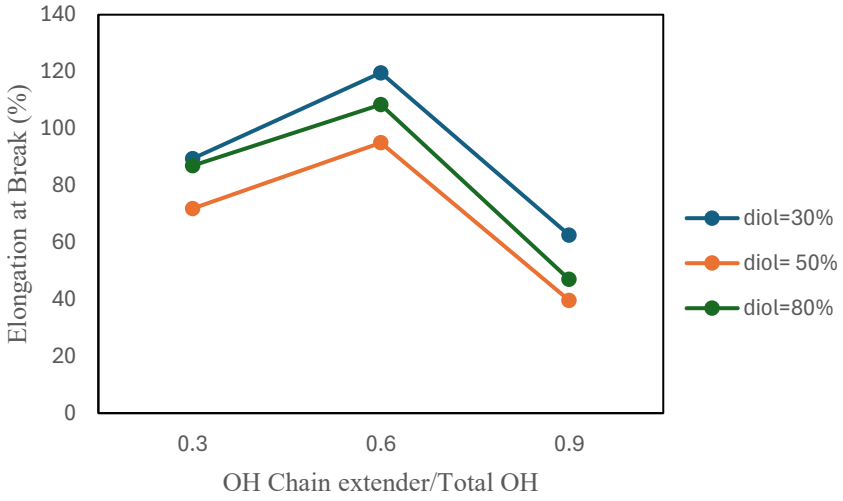

Figure 5. Elongation at break of the samples with different formulations.

4. Conclusions

This study investigated the effect of the diol polyol hydroxyl fraction (relative to the total polyol hydroxyl groups) and of the chain extender hydroxyl contribution on the structure and properties of two-component polyurethane roof coatings. Increasing the chain extender hydroxyl contribution promoted more developed microphase separation and raised both the storage modulus and tensile strength. The highest degree of microphase separation was observed at the highest chain extender hydroxyl fractions (0.9). Its effect on elongation at break was non-monotonic, peaking at the intermediate chain extender contribution (0.6). The highest degree of microphase separation was obtained at the highest diol polyol hydroxyl fraction (80%). As this fraction decreased, and the triol polyol hydroxyl fraction correspondingly increased, the higher density of chemical crosslinks acted as anchor points that restricted hard-segment mobility and limited hard-domain formation, lowering the degree of microphase separation and broadening the tan δ peaks. The broadest peak occurred at the 50% diol polyol hydroxyl fraction(intermediate diol hydroxyl fraction), where the crosslink density was high enough to partially restrict hard-domain formation but not to prevent it entirely, making this the most structurally heterogeneous formulation. The increased crosslink density nonetheless raised tensile strength and storage modulus, while elongation at break was lowest at the 50% diol polyol hydroxyl fraction due to this heterogeneity and highest at the lowest diol polyol hydroxyl fraction (30%). Overall, the formulation with a 30% diol polyol hydroxyl fraction and a chain extender ratio of 0.6 provided the best balance between mechanical strength and elongation at break, making it the most suitable candidate for roof coating applications.

6. References

[1] “Characteristics of membranes and insulations used for low-sloped roofs,” 2005.

[2] J. G. Lopes, J. R. Correia, and M. X. B. Machado, "Dimensional stability of waterproofing bituminous sheets used in low slope roofs," *Construction and Building Materials*, vol. 25, no. 8, pp. 3229–3235, Aug. 2011, doi: 10.1016/j.conbuildmat.2011.03.009.

[3] J. A. Marques, J. G. Lopes, and J. R. Correia, "Durability of the adhesion between bituminous coatings and self-protection mineral granules of waterproofing membranes," *Construction and Building Materials*, vol. 25, no. 1, pp. 138–144, Jan. 2011, doi: 10.1016/j.conbuildmat.2010.06.047.

[4] J. Feiteira, J. G. Lopes, and J. De Brito, "Mechanical Performance of Liquid-Applied Roof Waterproofing Systems," *J. Perform. Constr. Facil.*, vol. 27, no. 3, pp. 244–251, Jun. 2013, doi: 10.1061/(ASCE)CF.1943-5509.0000314.

[5] D. E. Fiori, "Two-component water reducible polyurethane coatings," *Progress in Organic Coatings*, vol. 32, no. 1–4, pp. 65–71, Dec. 1997, doi: 10.1016/S0300-9440(97)00076-3.

[6] M. Melchiors, M. Sonntag, C. Kobusch, and E. Jürgens, "Recent developments in aqueous two-component polyurethane (2K-PUR) coatings," *Progress in Organic Coatings*, vol. 40, no. 1–4, pp. 99–109, Dec. 2000, doi: 10.1016/S0300-9440(00)00123-5.

[7] F. E. Golling *et al.*, "Polyurethanes for coatings and adhesives – chemistry and applications," *Polymer International*, vol. 68, no. 5, pp. 848–855, May 2019, doi: 10.1002/pi.5665.

[8] C. Prisacariu, *Polyurethane Elastomers: From Morphology to Mechanical Aspects*. Vienna: Springer Vienna, 2011. doi: 10.1007/978-3-7091-0514-6.

[9] J. Wei *et al.*, "Enhanced mechanical strength and water resistance in waterborne polyurethanes through hydroxyl-functionalized MQ silicone resin modification," *Progress in Organic Coatings*, vol. 194, p. 108555, Sep. 2024, doi: 10.1016/j.porgcoat.2024.108555.

[10] J. Zhai, A. Pang, T. Ding, R. Liu, X. Guo, and T. Song, "Effect of crosslinking point structures on properties of polyurethane end-crosslinked PBT elastomers," *Iran Polym J*, vol. 31, no. 3, pp. 333–341, Mar. 2022, doi: 10.1007/s13726-021-00999-6.

[11] S. Wu, S. Ma, Q. Zhang, and C. Yang, "A comprehensive review of polyurethane: Properties, applications and future perspectives," *Polymer*, vol. 327, p. 128361, May 2025, doi: 10.1016/j.polymer.2025.128361.

[12] D. K. Chattopadhyay and K. V. S. N. Raju, "Structural engineering of polyurethane coatings for high performance applications," *Progress in Polymer Science*, vol. 32, no. 3, pp. 352–418, Mar. 2007, doi: 10.1016/j.progpolymsci.2006.05.003.

[13] K. Bagdi, K. Molnar, I. Sajo, and B. Pukanszky, "Specific interactions, structure and properties in segmented polyurethane elastomers," *Express Polym. Lett.*, vol. 5, no. 5, pp. 417–427, 2011, doi: 10.3144/expresspolymlett.2011.41.

[14] J. H. Silver, C. W. Myers, F. Lim, and S. L. Cooper, "Effect of polyol molecular weight on the physical properties and haemocompatibility of polyurethanes containing polyethylene oxide macroglycols," *Biomaterials*, vol. 15, no. 9, pp. 695–704, 1994, doi: 10.1016/0142-9612(94)90168-6.

[15] H. Wang *et al.*, "Effects of Isocyanate Structure on the Properties of Polyurethane: Synthesis, Performance, and Self-Healing Characteristics," *Polymers*, vol. 16, no. 21, p. 3045, Oct. 2024, doi: 10.3390/polym16213045.

[16] C. Tan, T. Tirri, and C.-E. Wilen, "Investigation on the Influence of Chain Extenders on the Performance of One-Component Moisture-Curable Polyurethane Adhesives," *Polymers*, vol. 9, no. 5, p. 184, May 2017, doi: 10.3390/polym9050184.

[17] B. Liu *et al.*, "Effect of hard segment content on the phase separation and properties of hydroxyl-terminated polybutadiene thermoplastic polyurethane," *Polymer Testing*, vol. 143, p. 108681, Feb. 2025, doi: 10.1016/j.polymertesting.2024.108681.

[18] L. P. Barros Junior, L. R. De Souza, R. Rahimzadeh, and I. Manas-Zloczower, "Improving performance of TPU by controlled crosslinking of soft segments," *Polymer Engineering & Sci*, vol. 64, no. 8, pp. 3982–3992, Aug. 2024, doi: 10.1002/pen.26826.

[19] P. Jutrzenka Trzebiatowska, A. Santamaria Echart, T. Calvo Correas, A. Eceiza, and J. Datta, "The changes of crosslink density of polyurethanes synthesised with using recycled component. Chemical structure and mechanical properties investigations," *Progress in Organic Coatings*, vol. 115, pp. 41–48, Feb. 2018, doi: 10.1016/j.porgcoat.2017.11.008.

[20] P. K. Saxena, K. G. Raut, S. R. Srinivasan, S. Sivaram, R. S. Rawat, and R. K. Jain, "Polyurethane waterproofing coating for building applications," *Construction and Building Materials*, vol. 5, no. 4, pp. 208–210, Dec. 1991, doi: 10.1016/0950-0618(91)90052-M.

[21] H. Huang *et al.*, "Influence of hard segment content and soft segment length on the microphase structure and mechanical performance of polyurethane-based polymer concrete," *Construction and Building Materials*, vol. 284, p. 122388, May 2021, doi: 10.1016/j.conbuildmat.2021.122388.

[22] Z. Yan, P. Yang, H. Yang, S. Zheng, and Z. Tan, "Influence of hard segment content on microphase separation and dielectric performance of polyurethane elastomers," *Colloid Polym Sci*, vol. 303, no. 11, pp. 2331–2342, Nov. 2025, doi: 10.1007/s00396-025-05489-2.

[23] A. J. Kosanovich, O. Jalife, Y. Fan, A. Shete, and Y. Srivastava, "Effects of polyether polyol hydroxyl equivalent weight on controlled release polyurethane coatings of urea (46-0-0)," *RSC Appl. Polym.*, vol. 4, no. 1, pp. 284–290, 2026, doi: 10.1039/D5LP00257E.

[24] S. M. Kang, S. J. Lee, and B. K. Kim, "Shape memory polyurethane foams," *Express Polym. Lett.*, vol. 6, no. 1, pp. 63–69, 2012, doi: 10.3144/expresspolymlett.2012.7.

[25] S. Yang, S. Zhai, M. Piao, X. Wang, H. Shi, and C. Li, "Analysis of Water-Based Polyurethane Properties in the Ballistic Behavior of Ultra-High Molecular Weight Polyethylene Fiber Composites," *Polymers*, vol. 17, no. 7, p. 837, Mar. 2025, doi: 10.3390/polym17070837.

[26] S. Velankar and S. L. Cooper, "Microphase Separation and Rheological Properties of Polyurethane Melts. 1. Effect of Block Length," *Macromolecules*, vol. 31, no. 26, pp. 9181–9192, Dec. 1998, doi: 10.1021/ma9811472.

[27] B.-X. Cheng *et al.*, "A review of microphase separation of polyurethane: Characterization and applications," *Polymer Testing*, vol. 107, p. 107489, Mar. 2022, doi: 10.1016/j.polymertesting.2022.107489.

[28] P. Somdee, T. Lassu-Kuknyo, C. Konya, T. Szabó, and K. Marossy, "Investigating the Properties and Structure of Polyurethane Elastomers with Monoethylene Glycol Chain Extender," *MSF*, vol. 986, pp. 18–23, Apr. 2020, doi: 10.4028/www.scientific.net/MSF.986.18.

[29] Y. Wang *et al.*, "Understanding water absorption effect on molecular dynamics, microstructures and relaxation behavior of segmented polyurethane elastomers," *Polymer Degradation and Stability*, vol. 214, p. 110415, Aug. 2023, doi: 10.1016/j.polymdegradstab.2023.110415.